

## Electronic Supplementary Information

to

# Extremely Robust and Post-Functionalizable Gold Nanoparticles Coated with Calix[4]arenes via Metal-Carbon bonds

Ludovic Troian-Gautier, Hennie Valkenier, Alice Mattiuzzi, Ivan Jabin, Niko Van den  
Brande, Bruno Van Mele, Julie Hubert, François Reniers, Gilles Bruylants, Corinne Lagrost  
and Yann Leroux

|                                                                        |       |
|------------------------------------------------------------------------|-------|
| 1. Instrumentation                                                     | p.S2  |
| 2. Synthesis of compound <b>2</b> and of functionalized AuNPs <b>3</b> | p.S4  |
| 3. Transmission Electron Microscopy                                    | p.S9  |
| 4. Thermogravimetric analyses                                          | p.S12 |
| 5. X-ray Photoelectron Spectroscopy                                    | p.S16 |
| 6. UV-Visible spectra as function of pH                                | p.S17 |
| 7. AuNP stability studies                                              | p.S20 |
| 8. Post-functionalization                                              | p.S25 |
| References                                                             | p.S27 |

## 1. Instrumentation.

The  $^1\text{H}$  NMR,  $^{13}\text{C}$  NMR and 2D NMR spectra were recorded with a Bruker Avance-300 instrument and a Varian-400 VNMRJ System. The chemical shifts are expressed in ppm relative to the deuterated solvent used as internal reference. Most of the  $^1\text{H}$  NMR spectra signals were attributed through 2D NMR analyses (COSY, HSQC, HMBC).

The electronic absorption spectra were recorded with a Perkin-Elmer Lambda UV-Vis or a Shimadzu UV3600 spectrophotometer.

The thermogravimetric analyses (TGA) were performed by 2 different methods: *Method I (Mass versus temperature)* on a Perkin Elmer Pyris 6 TGA device. For this purpose, 4 to 6 mg of the material weighed in a ceramic crucible Perkin Elmer TGA undergo a linear ramp of increasing temperature up to  $550^\circ\text{C}$  at a rate of  $10^\circ\text{C}\cdot\text{min}^{-1}$  under nitrogen inert atmosphere. The obtained results are then processed with the Pyris Manager software.

*Method II (Mass versus time)*, on a TA Instruments Q5000 TGA with air as purge gas ( $25\text{ mL}\cdot\text{min}^{-1}$ ). A suspension of AuNPs in  $150\text{-}400\ \mu\text{L}$  water was placed in a DSC crucible and the water was evaporated in a vacuum oven by slowly decreasing the pressure and increasing the temperature. When the dark red liquid had turned into a gold colored film, the crucible was further dried for 30 minutes at 10 mbar and  $75^\circ\text{C}$ . The crucible was loaded in the TGA instrument and a 2 h isotherm was measured at  $60^\circ\text{C}$ , followed by a linear ramp up to  $600^\circ\text{C}$  at a rate of  $10^\circ\text{C}\cdot\text{min}^{-1}$ , a 30 or 60 min isotherm at  $600^\circ\text{C}$ , cooling, and another 2 h isotherm at  $60^\circ\text{C}$ . The loss of organic material was obtained by the difference in weight at the plateaus of the  $60^\circ\text{C}$  isotherms before and after heating.

XPS measurements were performed on a PHI 5600 instrument. All spectra were acquired using the Mg  $K\alpha$  X-ray source ( $h\nu = 1253.6\text{ eV}$ ) operating at 300 W with a  $45^\circ$  take-off angle (TOA). Here the photoelectron TOA is defined as the angle between the surface normal and the axis of the analyzer lens. Survey spectra ( $0\text{-}1100\text{ eV}$ ) were acquired with an analyzer pass energy of  $187.85\text{ eV}$  (dwell time =  $0.05\text{ s}$ ,  $1\text{ eV}/\text{step}$ , #scan = 4). Binding energies were referenced to the C1s peak at  $285\text{ eV}$ . The spot size was set to a diameter of  $400\ \mu\text{m}$ . The atomic concentration for surface composition was estimated using the integrated peaks areas, normalized by the manufacturer supplied sensitivity factor. The composition was calculated using the average value of 3 measurements on individual spots for each sample. (Casa Software, Ltd. version 2.3.15).

TEM experiments were carried out either with a JEOL 2100 LaB6 microscope operating at 200KV on which the images were recorded on a GATAN Orius 200D CCD camera or with a Philips CM20-UltraTWIN microscope.

FTIR spectra were recorded, at room temperature, with a Bruker IFS 25 FTIR spectrophotometer at a nominal resolution of  $2\text{ cm}^{-1}$  and encoded every  $1\text{ cm}^{-1}$  or by using a Bruker Vertex 70 spectrometer (200 scans were collected and averaged).

## 2. Synthesis of compound 2 and of functionalized AuNPs 3

**Chemicals.** Solvents and reagents for the syntheses were at least of reagent grade quality and were used without further purification. The reaction mixtures containing aryl diazonium salts were protected from direct light during the synthesis and work-up to prevent photo-degradation.

*Caution!* Although we have not encountered any problem, it is noted that diazonium salts derivatives are potentially explosive and should be handled with appropriate precautions.

**Synthesis of calix[4]arene-tetra-diazonium 2.** Calix[4]arene-tetra-aniline **1**<sup>1</sup> (0.200 g, 0.207 mmol, 1 equiv.) was solubilized in acetonitrile (1.5 mL) and NOBF<sub>4</sub> (0.129 g, 0.549 mmol, 5 equiv.) was added at -40°C under Ar. After 2h, the mixture was centrifuged and the precipitate was washed with acetonitrile (3 x 1 mL). The supernatant were combined and concentrated under reduced pressure to yield the compound **2** as a yellow solid (0.149 g, 0.19 mmol, 98%). IR:  $\nu$ : 3060, 2991, 2261, 1267, 1037 cm<sup>-1</sup>; <sup>1</sup>H NMR (300 MHz, CD<sub>3</sub>CN, 298K):  $\delta_{(\text{ppm})}$  = 3.80 (d, <sup>2</sup>J = 14.7 Hz, 4H, ArCH<sub>2eq</sub>), 4.96-5.08 (m, 12H, OCH<sub>2</sub> + ArCH<sub>2ax</sub>), 8.07 (s, 8H, ArH); <sup>13</sup>C NMR (75 MHz, CD<sub>3</sub>CN, 298K):  $\delta_{(\text{ppm})}$  = 31.7, 73.0, 109.5, 135.7, 138.7, 167.3, 170.2.

HRMS analysis was not performed because of the low stability of the compound **2** against temperature.

## 1D and 2D NMR spectra of compound 2.

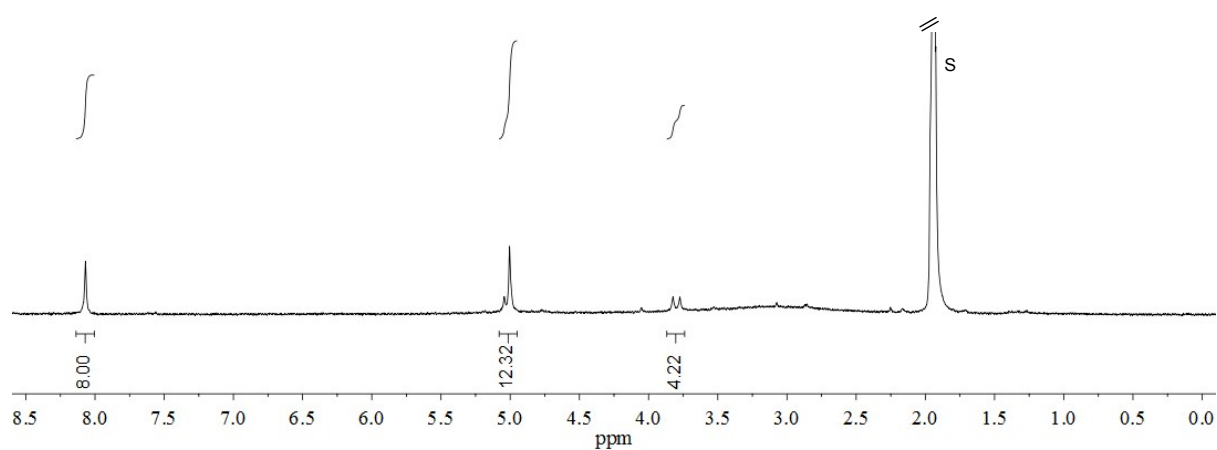


**Figure S1.** <sup>1</sup>H NMR spectrum of compound 2 (300 MHz, CD<sub>3</sub>CN, 298K). S = solvent.

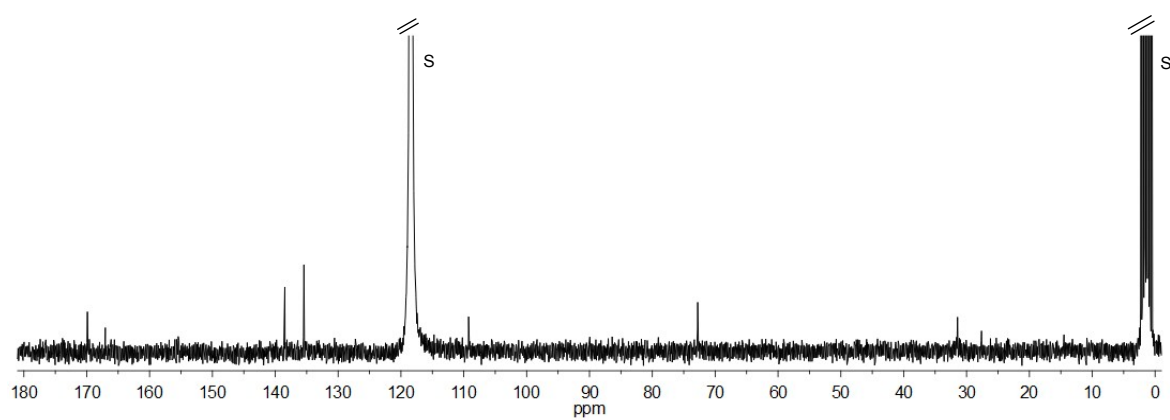


**Figure S2.** <sup>13</sup>C NMR spectrum of compound 2 (75 MHz, CD<sub>3</sub>CN, 298K). S = solvent.

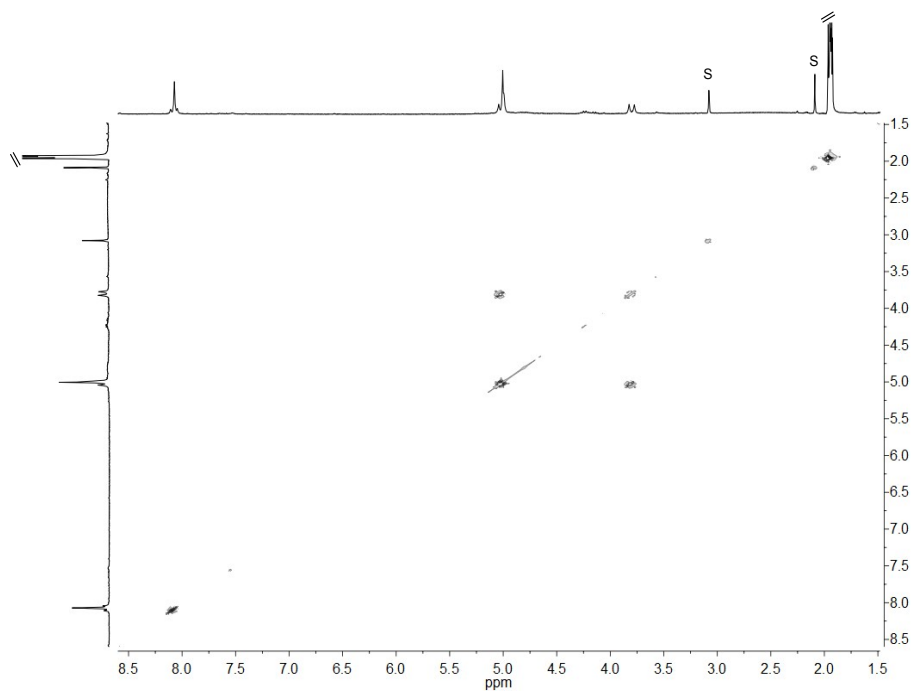


**Figure S3.** COSY NMR spectrum of compound 2 (300 MHz, CD<sub>3</sub>CN, 298K).

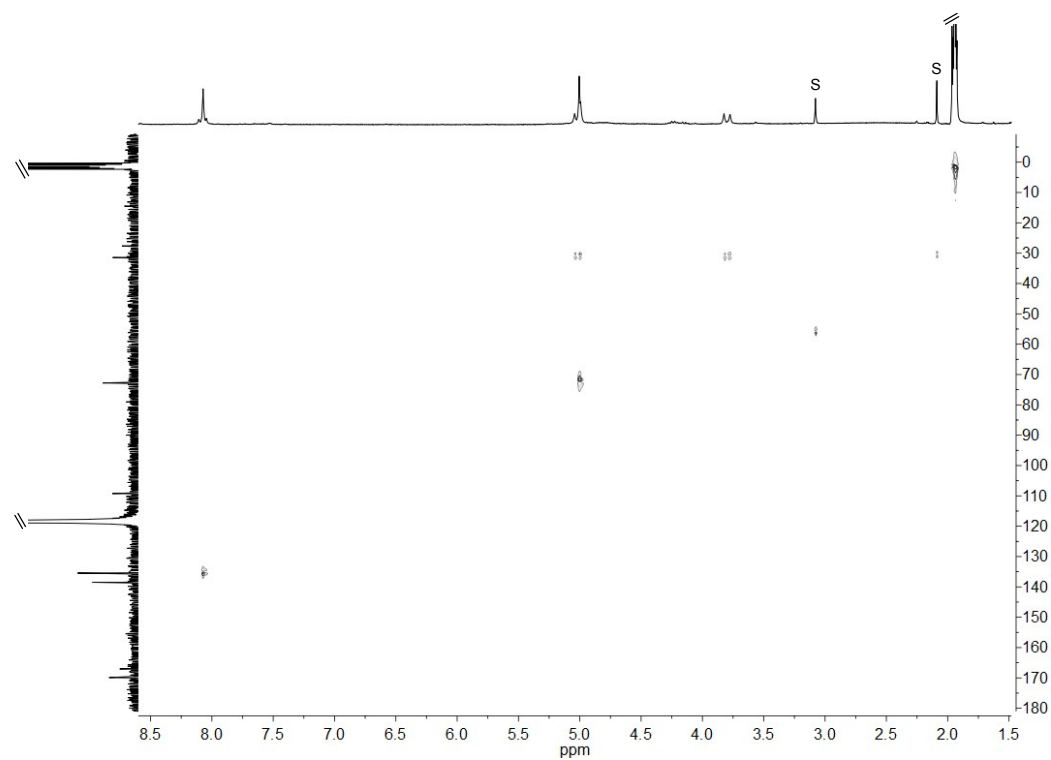


**Figure S4.** HSQC NMR spectrum of compound **2** (400 MHz, CD<sub>3</sub>CN, 298K).

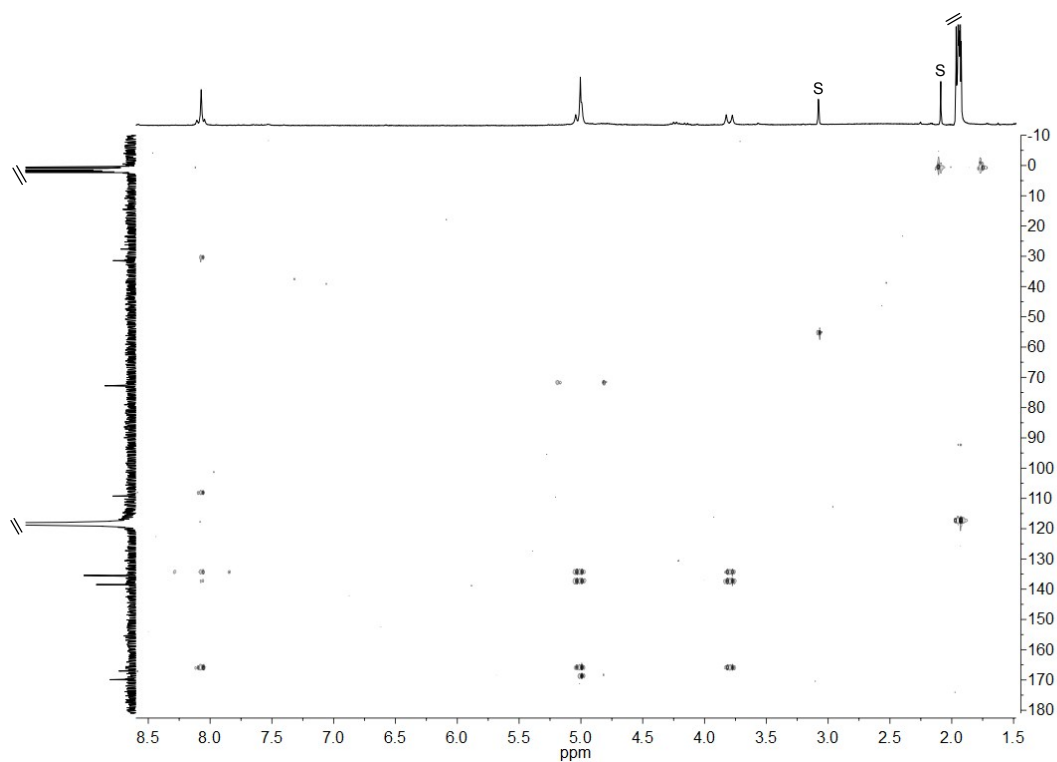


**Figure S5.** HMBC NMR spectrum of compound **2** (400 MHz, CD<sub>3</sub>CN, 298K).

**Synthesis of gold nanoparticles 3a in presence of calix[4]arene-tetra-diazonium salt 2.** HAuCl<sub>4</sub>·3H<sub>2</sub>O (25 mg, 0.0635 mmol, 1 equiv.) was dissolved in acetonitrile (25 mL) and a solution of calix[4]arene-tetra-diazonium salt **2** (24 mg, 0.0315 mmol, 0.5 equiv.) in acetonitrile (25 mL) was added. The reaction mixture was stirred vigorously at 0°C under Ar and an aqueous solution of NaBH<sub>4</sub> (0.5 mL, 6.1 mg, 0.161 mmol, 2.5 equiv.) was added dropwise. The color of the reaction mixture changed from yellow to dark ruby. After 2 hours of vigorous stirring, the reaction mixture was centrifuged at 5000 rpm for 20 min. The gold nanoparticles were washed by resuspension in NaOH (1 M) and precipitation with HCl (1 M) (two centrifugation cycles using 30 mL) and with water (1 × 30 mL) to obtain gold nanoparticles **3a** stabilized by calix[4]arenes (18 mg). The gold nanoparticles **3a** were dispersed in NaOH (1 M, 40 mL) and stored at 4°C for several weeks, without exhibiting any noticeable aggregation.

**15 nm calixarene-stabilized AuNPs 3b by grafting of 2.** AuNPs were synthesized as reported previously using a modified Turkevich method<sup>2,3</sup> and dialyzed against a 1 mM solution of citrate. To the resulting gold nanoparticles (15-19 nm depending on the batch, 24 mL, 25 nM, 0.6 nmol) was added a solution of NaBH<sub>4</sub> (100 µL, 0.3 M, 0.030 mmol)<sup>1</sup> in water, followed by the slow addition of a solution of calix[4]arene-tetra-diazonium salt **2** (45.9 mg, 0.060 mmol) in water (6 mL), resulting in effervescence of the red colloidal suspension. The reaction mixture was stirred overnight at room temperature, followed by the centrifugation of the mixture. The functionalized AuNPs **3b** were resuspended in 1 mM NaOH and collected by centrifugation (30 min at 15000 rpm) 6 times. For the TGA experiments, the AuNPs were washed an additional 4 times with water. AuNPs **3b** were stored in water at room temperature.

**10 nm calixarene-stabilized AuNPs 3c by grafting of 2.** To 1 mL of a dispersion of commercially available citrate-stabilized gold nanoparticles (10 nm, Aldrich, 9.9 nM) was added 1 mg of calix[4]arene-tetra-diazonium **2** previously dissolved in 1 mL of acetonitrile at room temperature and under stirring. The reaction mixture was stirred overnight at room temperature, and then centrifuged at 5000 rpm for 20 min. The gold nanoparticles were

---

<sup>1</sup> The addition of NaBH<sub>4</sub> raises the pH of the AuNPs suspension from 7.4 to 9, preventing aggregation of AuNPs upon addition of the acidic dispersion of **2**. The addition of NaOH instead of NaBH<sub>4</sub> also stabilized the AuNP suspension, but resulted in less robust AuNPs upon reaction with **2**, indicating that the reduction of diazonium groups by NaBH<sub>4</sub> is aiding the efficient functionalization of the AuNPs.

washed twice with 1 M HCl to obtain gold nanoparticles **3c** stabilized by calix[4]arenes. The gold nanoparticles **3c** were dispersed in NaOH (1 M, 2 mL).

**5 nm calixarene-stabilized AuNPs 3d by grafting of 2.** To 1 mL of a dispersion of commercially available citrate-stabilized gold nanoparticles (5 nm, Aldrich, 91 nM) was added 9.3 mg of calix[4]arene-tetra-diazonium **2** previously dissolved in 1 mL of acetonitrile at room temperature and under stirring. The reaction mixture was stirred overnight at room temperature, and then centrifuged at 5000 rpm for 20 min. The gold nanoparticles were washed twice with 1 M HCl to obtain gold nanoparticles **3d** stabilized by calix[4]arenes. The gold nanoparticles **3d** were dispersed in NaOH (1 M, 2 mL).



### 3. Transmission Electron Microscopy

#### Discussion of the synthesis of AuNPs **3a** and TEM results (Fig. 1)

From a mechanistic point of view, aurate salts and aryl diazonium salts are both chemically reduced in the acetonitrile solution, forming respectively gold clusters and aryl radicals. The order in which these reactions occur is still unknown but it is reasonable to assume that the grafting of calix[4]arenes results in the inhibition of nanoparticles growth, similarly to what is observed for AuNPs stabilized by thiol-based ligands. The size dispersity of the AuNPs **3a** is slightly less uniform than that reported for the AuNPs obtained by Schiffrin and coworkers (average diameter of  $8.1 \pm 0.8$  nm).<sup>4</sup> Main differences in the synthetic protocols could explain this discrepancy. First, Schiffrin and coworkers have used molecules bearing just one aryl diazonium function whereas the calix[4]arenes employed in this study possess four aryl diazonium functions with a constrained geometry that can affect their reactivity. Furthermore, they used an aryl diazonium salt with a long alkyl chain that can act as a phase transfer agent. Thus, the dispersity of the AuNPs obtained by Schiffrin and coworkers could have been greatly influenced by a pre-organization of the aurate and aryl diazonium salts in the toluene phase. At last, in their synthetic protocol, Schiffrin and coworkers have purified the AuNPs using a silica chromatographic column. Even if this purification step was performed mainly to separate AuNPs from soluble impurities, it can also impact AuNPs size uniformity. However, it is worth noting that many other examples in the literature<sup>5,6,7,8</sup> have reported on the formation of non-uniform nanoparticles upon the use of aryl diazonium reduction chemistry, in agreement with the high reactivity of aryl radicals.

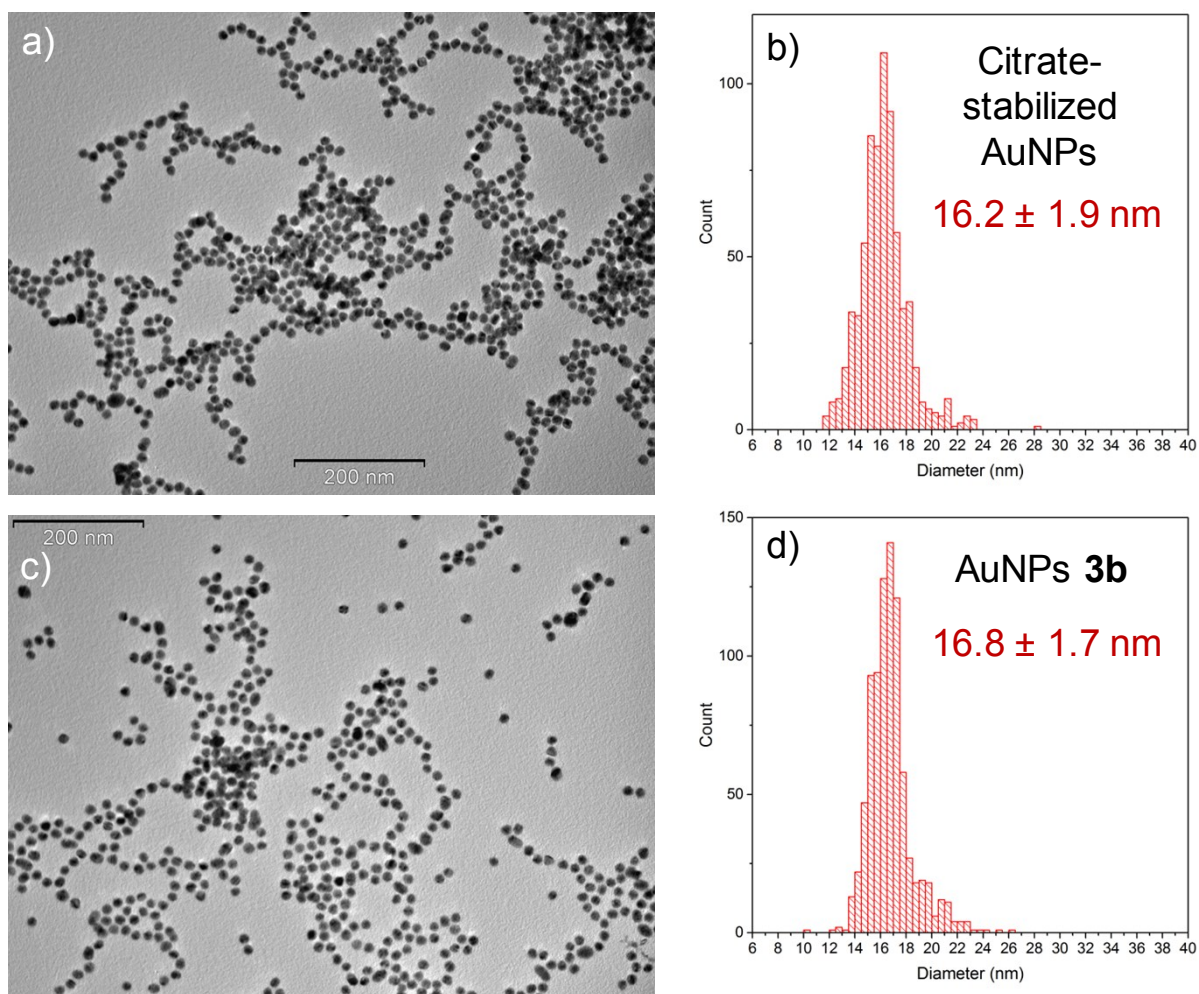


**Figure S6.** a, c) TEM micrographs and b, d) corresponding particle core size histogram<sup>9</sup> of in-house synthesized citrate-stabilized AuNPs before (a, b) and after (c, d) grafting of calix[4]arene-tetra-diazonium **2** to give AuNPs **3b**. No significant change in the size or shape of the AuNPs was observed upon grafting **2**.

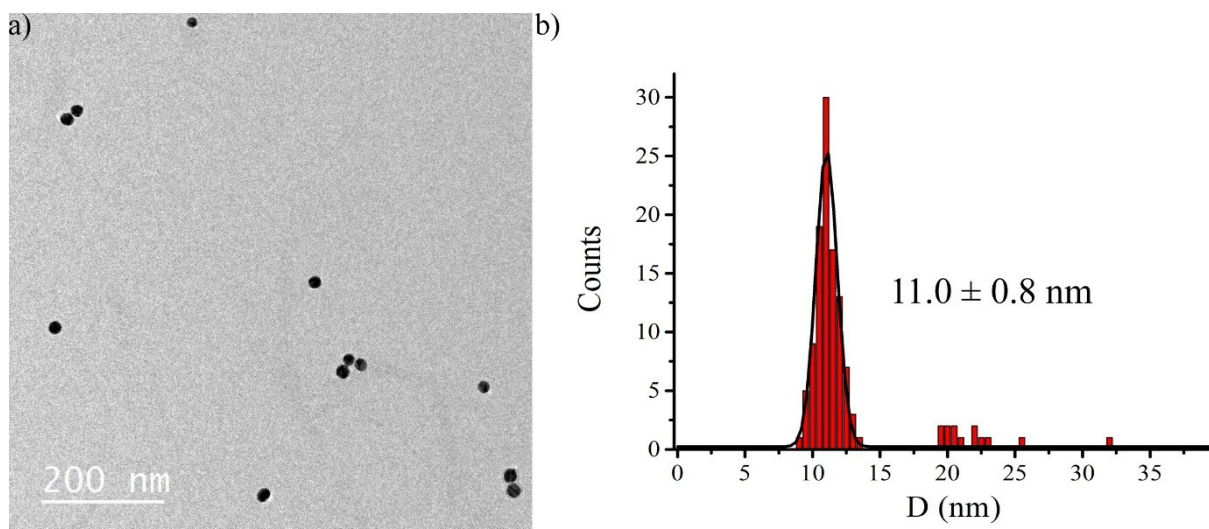


**Figure S7.** a) TEM micrographs and b) corresponding particle core size histogram for AuNPs obtained by spontaneous grafting of **2** on 10 nm citrate-stabilized AuNPs giving AuNPs **3c**.

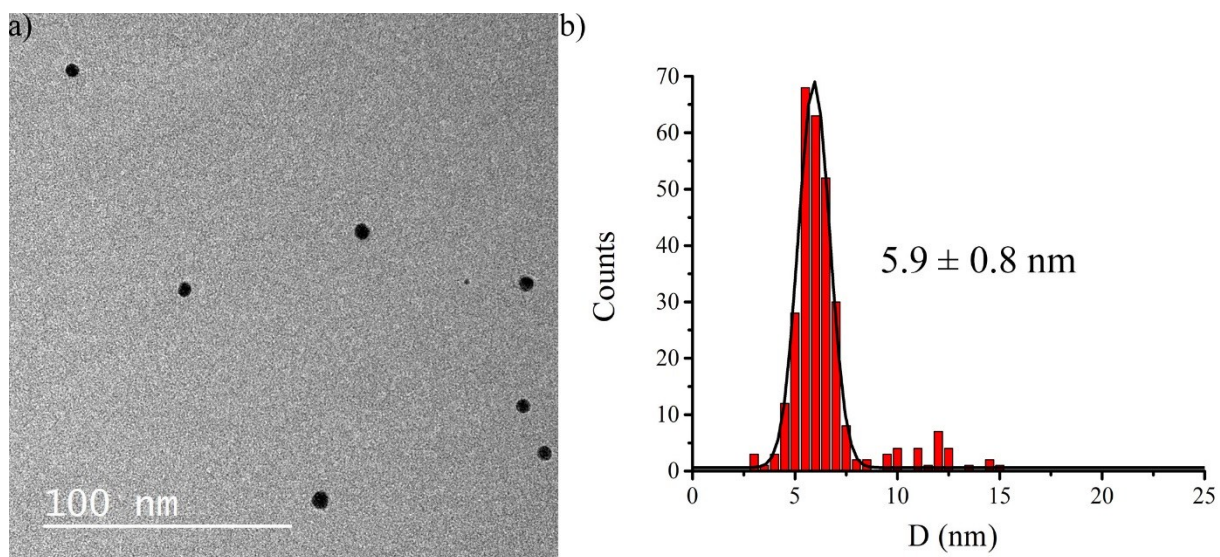


**Figure S8.** a) TEM micrographs and b) corresponding particle core size histogram for AuNPs obtained by spontaneous grafting of **2** on 5 nm citrate-stabilized AuNPs giving AuNPs **3d**.

#### 4. Thermogravimetric analyses of compound **2** and AuNPs **3a** and **3b**

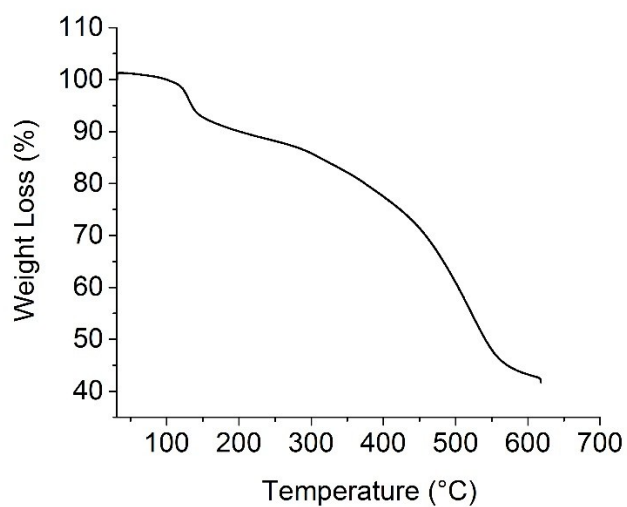


**Figure S9.** Thermogravimetric analysis of compound **2**, using method I.

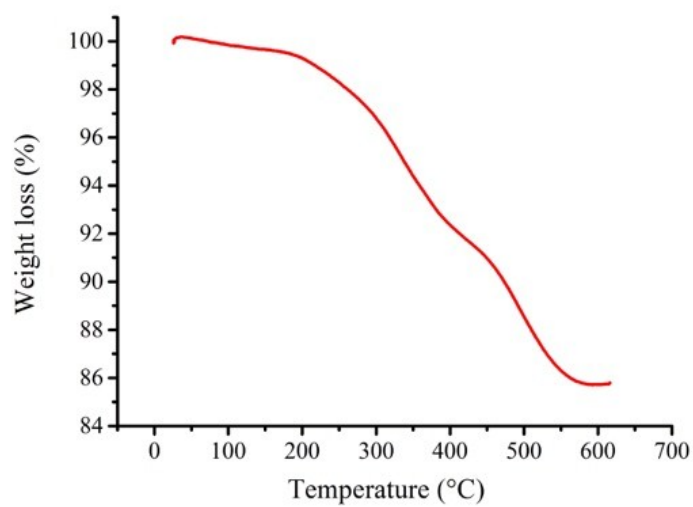


**Figure S10.** Thermogravimetric analysis of AuNPs **3a** (first batch) using method I.

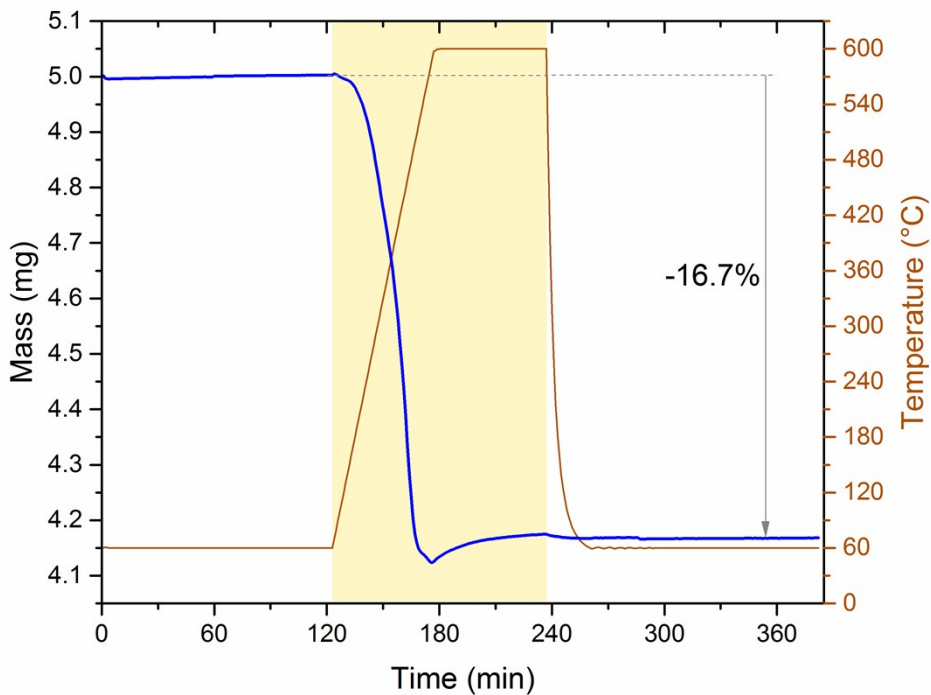


**Figure S11.** Thermogravimetric analysis of AuNPs **3a** (second batch) using method II.

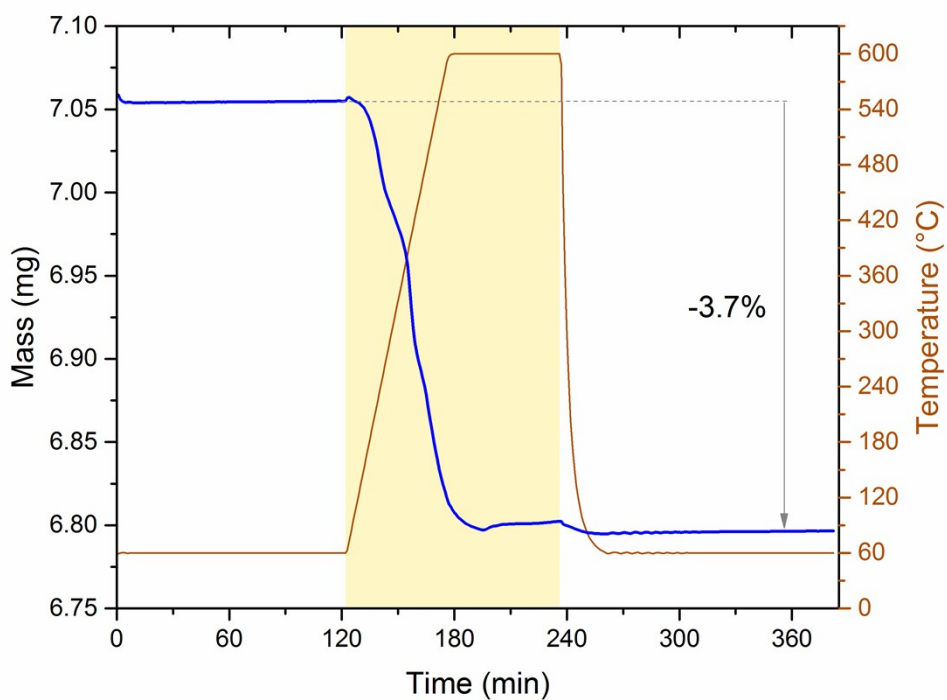


**Figure S12.** Thermogravimetric analysis of AuNPs **3b** (first batch) using method II.

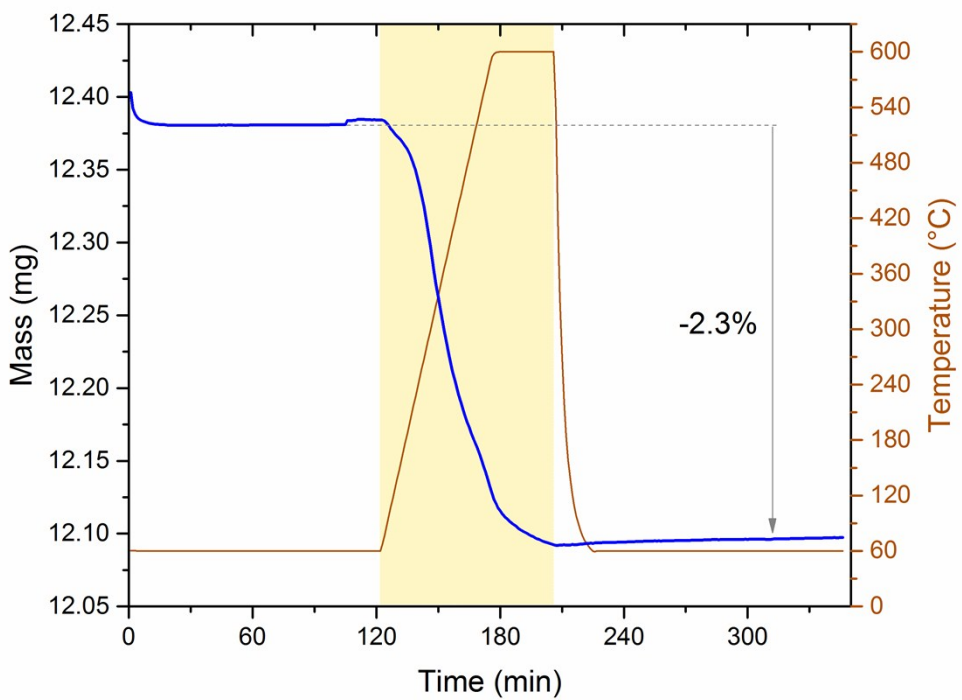


**Figure S13.** Thermogravimetric analysis of AuNPs **3b** (second batch) using method II.

The TGA data were used to determine the grafting density of the calixarenes on the surface of the AuNPs. From TEM experiments, it is possible to estimate the number of gold atoms constituting each nanoparticle, following equation (1):<sup>7</sup>

$$N_{Au} = \frac{\pi}{6} d D^3 \quad (1)$$

where  $N_{Au}$  is the number of gold atoms,  $d$  the density of gold ( $59 \times 10^{21}$  atoms.cm<sup>-3</sup> for face-centered cubic gold), and  $D$  the diameter in nm of the nanoparticles.

Since the molar mass of gold is 197 g.mol<sup>-1</sup>, the weight of the gold core ( $W_{Au}$ ) is given by equation (2):

$$W_{Au} = N_{Au} \times 197 \quad (2)$$

The value of  $W_{Au}$  found with equation (2) can be correlated with the percentage of gold atoms found in TGA measurements. Knowing the molar mass of the calix[4]arene (here assumed to be 652.6 g.mol<sup>-1</sup> when bound to a gold surface), it is thus possible to determine the number of ligands per nanoparticle and the density of the calixarenes on the surface of the AuNPs.

**Table S1. Structural parameters of AuNPs 3, determined from TEM and TGA analyses.**

| NP           | Particle diameter [nm] | Au [%] | No. of calix / Np | No. of calix / nm <sup>2</sup> | Comment   |
|--------------|------------------------|--------|-------------------|--------------------------------|-----------|
| <b>3a.I</b>  | 6.1 ± 1.9              | 85.8   | 350               | 3.0                            | Method I  |
| <b>3a.II</b> | 6.3 ± 2.2              | 83.3   | 478               | 3.8                            | Method II |
| <b>3b.I</b>  | 15.8 ± 2.7             | 96.3   | 1389              | 1.8                            | Method II |
| <b>3b.II</b> | 18.6 ± 4.2             | 97.7   | 1422              | 1.3                            | Method II |

## 5. X-ray Photoelectron Spectroscopy

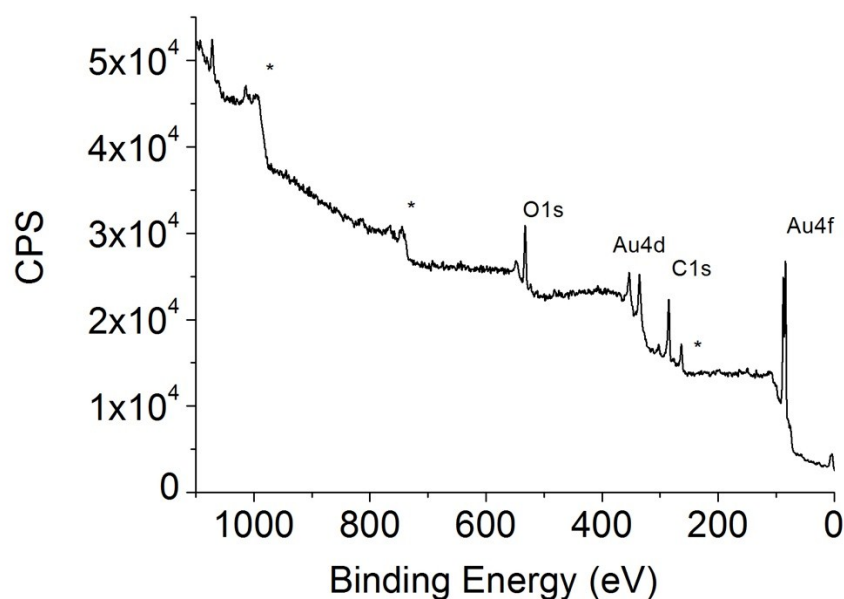


**Figure S14.** XPS survey spectra of AuNPs **3a**. (\*Auger peaks)

The survey spectra on AuNPs **3a** display peaks corresponding to elemental species C (C1s at 285 eV), O (O1s at 533 eV), Au (Au4f at 84 eV) for AuNPs **3a**. The binding energies observed for Au4f peaks doublet (84 eV for Au4f<sub>7/2</sub> and 87.8 eV for Au4f<sub>5/2</sub>) match with the expected values for Au<sup>0</sup>. The complete conversion of Au<sup>3+</sup> to Au<sup>0</sup> is further assessed by the absence of Au4f peak at 86.0 eV. Likewise, the absence of the N1s peak at 404 eV characteristic of a diazonium group shows the complete reaction of the diazonium salts. The peaks corresponding to C1s and O1s photoelectrons can be mainly assigned to the calix[4]arene ligands.

The chemical composition (atom %) for the AuNPs **3a** was found to be 7% Au, 69% C, 22% O and 2% Na ( $\pm 20\%$ ), clearly reflecting the 3:1 ratio between C and O in the molecular formula of **2** (C<sub>36</sub>H<sub>24</sub>N<sub>8</sub>O<sub>12</sub>Na<sub>4</sub>). The observation of Na can be attributed to the presence of Na<sup>+</sup> counter ions in the XPS sample.



## 6. UV-Visible spectra as function of pH

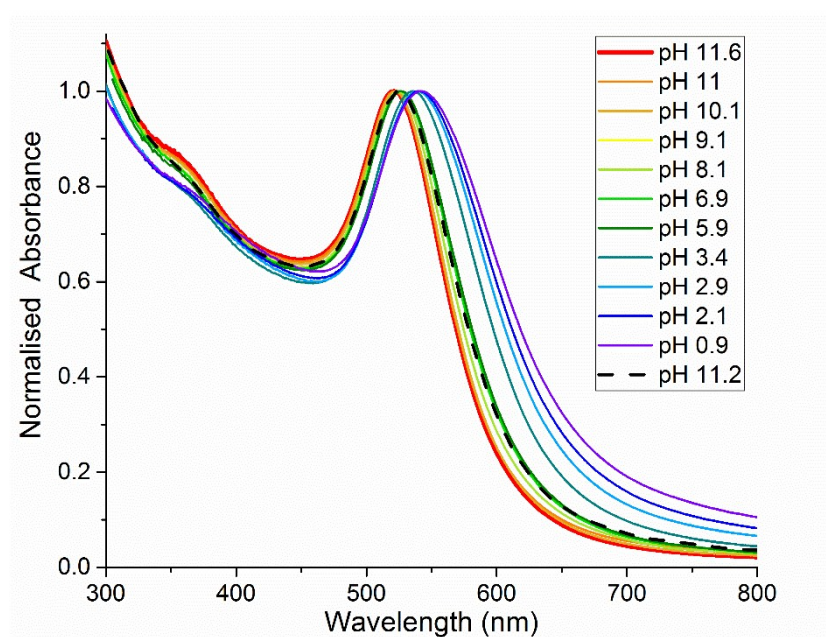


**Figure S15.** UV-Visible spectra of AuNPs **3c** (synthesized by spontaneous grafting of calix[4]arene-tetra-diazonium **2** with commercially available 10 nm citrate-stabilized AuNPs) in HEPES buffer at pH 11.6 (red) down to pH 0.9 (violet) and then back to pH 11.2 (black dashed).

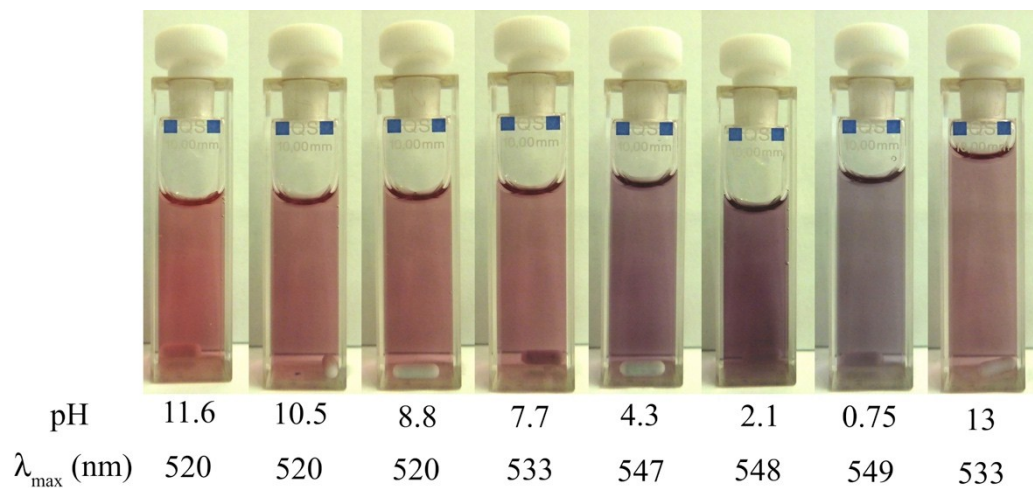


**Figure S16.** Photos of colloidal dispersions of AuNPs **3a** in HEPES buffer adjusted to various pH values. The wavelengths of the plasmon band absorption maxima  $\lambda_{\max}$  are depicted.

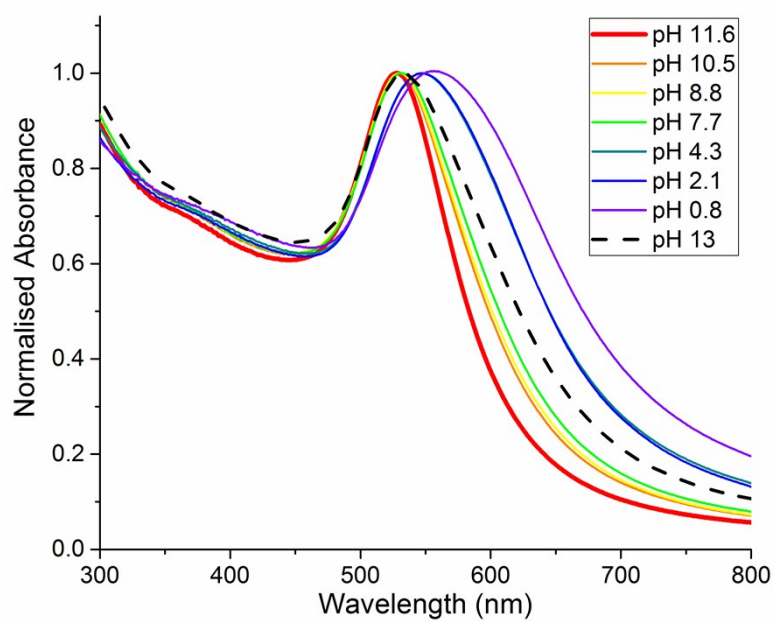


**Figure S17.** UV-Visible spectra of AuNPs **3a** in HEPES buffer at pH 11.6 (red) down to pH 0.8 (violet) and then back to pH 13 (black dashed).

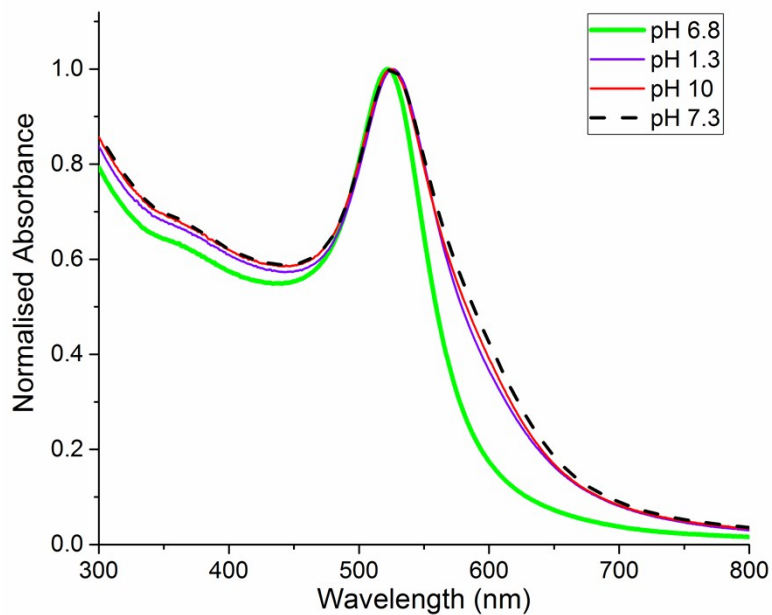


**Figure S18.** UV-Visible spectra of commercial 5 nm citrate-stabilized AuNPs at pH 6.8 (as-received, green curve) then acidified to pH 1.3 (violet) followed by basification to pH 13 (red) and neutralization back to pH 7.3 (black dashed).

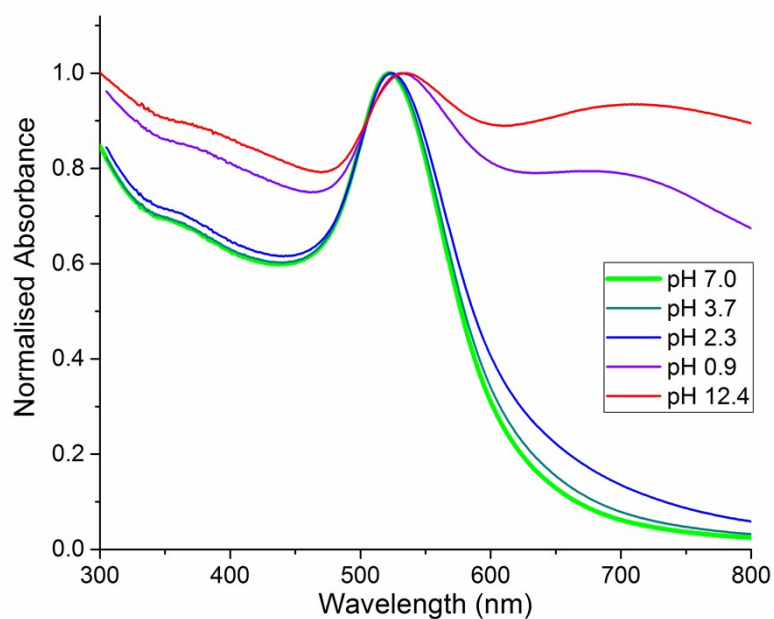


**Figure S19.** UV-Visible spectra of 15 nm citrate-stabilized AuNPs at pH 7.0 (green curve) then gradually acidified to pH 0.9 (violet) followed by basification to pH 12.4 (red).

## 7. AuNP stability studies.

### Drying of the AuNPs into a film and resuspension

Similar to the experiment described in Fig 3b of the main text for AuNPs **3a**, also AuNPs **3b** were dried into a gold colored film and successfully resuspended in 0.1 M NaOH.

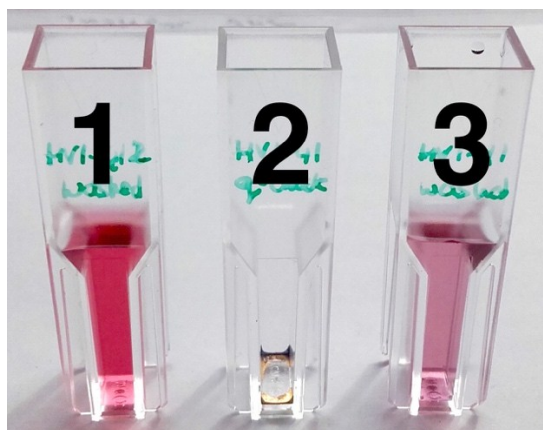


**Figure S20.** Photo of calix-AuNPs **3b** suspended in water (1), allowed to dry into a gold-colored film (2), and after resuspension in 0.1 M NaOH (3).

### Stability of AuNPs **3a** and **3b** towards fluoride

The stability of AuNPs was tested by addition of fluoride to the AuNPs dispersions. The AuNPs used in this study were soluble in different solvents. AuNPs stabilized by Au-C bonds (synthesized in the presence of 4-diazonium decylbenzene, as described by Schiffrin)<sup>4</sup> were dispersed in toluene and dodecanethiol-capped AuNPs in THF. AuNPs **3a** and **3b** were dispersed in water, just as the synthesized 15 nm citrate-stabilized AuNPs. Hence, two different fluoride solutions were prepared: a solution of tetrabutylammonium fluoride (TBAF) in THF (0.5 M) and a solution of KF in water (4 M). Thiol-capped AuNPs synthesized in this study have a concentration of  $5.3 \times 10^{-8}$  M and were used at this concentration. The concentration of AuNPs stabilized by Au-C bonds using Schiffrin's synthetic methodology was adjusted to  $1.3 \times 10^{-8}$  M using UV-Visible measurements. The validity of the equation used to calculate the AuNPs concentration developed by Huo *et al.*<sup>10</sup> was tested by using the commercially available citrate-stabilized AuNPs. A variation of less than 10% was found between the concentration announced by the manufacturer and the one found by UV-Visible measurements. AuNPs **3a** and **3b** and citrate stabilized AuNPs were used at an optical density of  $\sim 1$ , corresponding to  $\sim 2.5 \times 10^{-9}$  M for the latter two sets of 15 nm AuNPs.

The stability tests were performed by adding  $2 \times 10^{-4}$  mol (0.4 mL) of TBAF solution to the AuNPs in organic solvents (blue dashed curves in Figure S21) or by adding 39  $\mu$ L of a 4 M KF solution to the AuNPs in water, both resulting in a final fluoride concentrations of 0.15 M. Since no aggregation was observed for AuNPs **3a** and **3b**, the fluoride concentration was further increased to 0.30 M (green dotted curves).

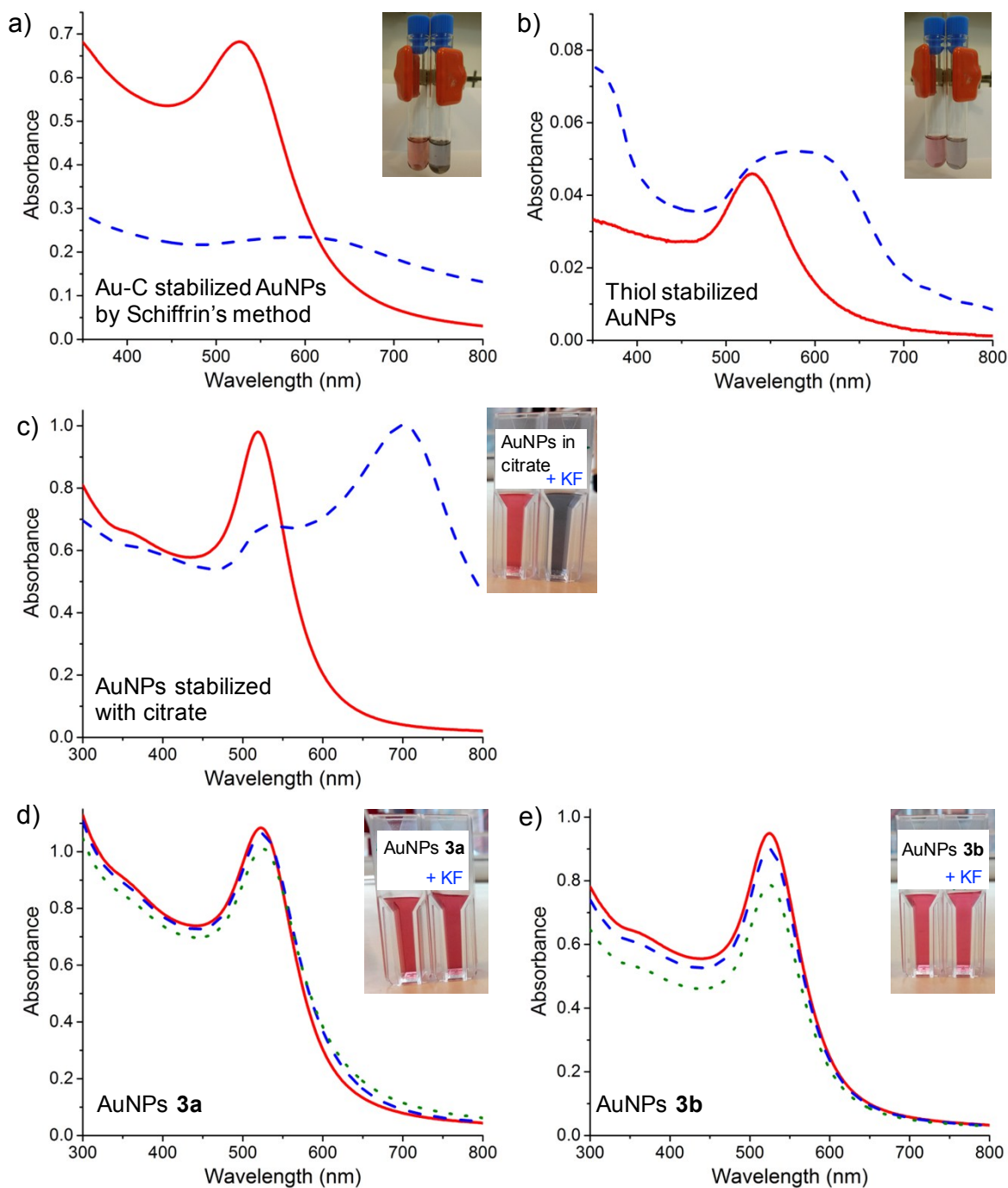


**Figure S21.** UV-Visible Spectra of a) AuNPs stabilized by Au-C bonds following Schiffrin's synthetic methodology (in toluene), b) AuNPs capped with dodecanethiol (in THF), c) citrate-stabilized AuNPs (in water), d) calix[4]arene stabilized AuNPs **3a** (in water), e) calix[4]arene stabilized AuNPs **3b** (in water). Red lines correspond to UV-Visible spectra of AuNPs before addition of fluoride, blue dashed lines after addition of fluoride (0.15 M final concentration), and green dotted lines after addition of 0.30 M fluoride to **3a** and **3b**. Photos are shown of the AuNP dispersions before and after (the first) addition of fluoride.

## Stability of AuNPs 3a and 3b in NaCl solution

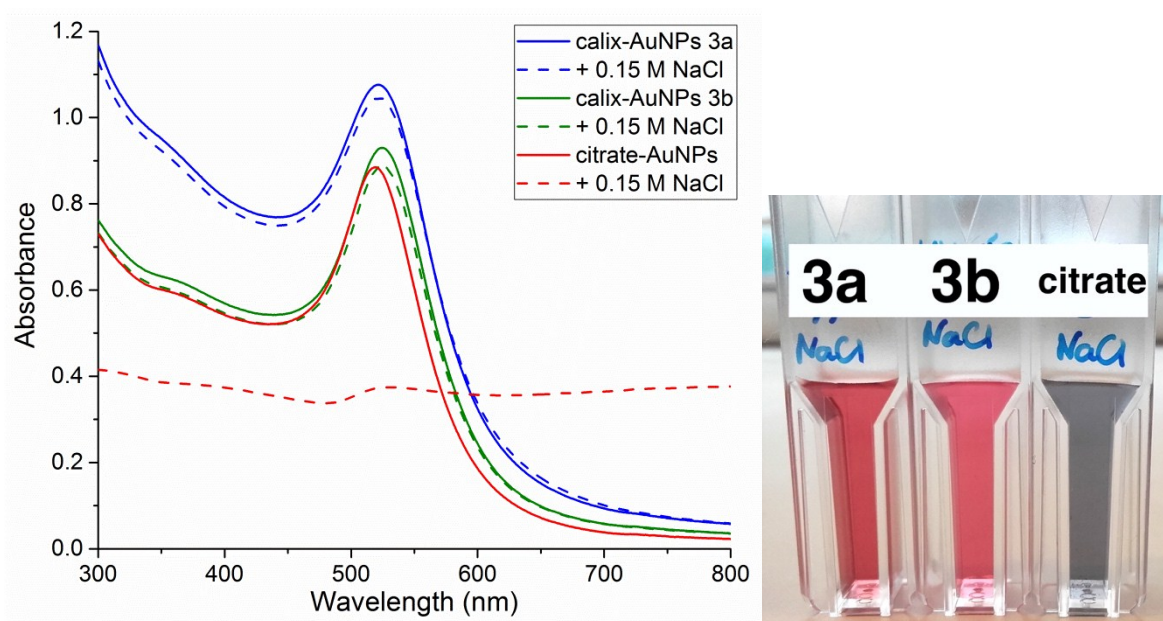


**Figure S22.** UV-Visible spectra of aqueous dispersions of calix-AuNPs **3a** (blue), calix-AuNPs **3b** (red), and 15 nm AuNPs in 1 mM citrate (green). 39  $\mu$ L of a 4 M NaCl solution were injected into each of these AuNP suspensions to get a concentration of 0.15 M NaCl. The UV-Vis spectra recorded after injection of NaCl (dashed) show strong aggregation of the citrate-protected AuNPs, whereas no change is observed for the calixarene-functionalized AuNPs **3a** and **3b**. The photo shows the AuNP dispersions after addition of NaCl.

### Stability of AuNPs 3a and 3b in phosphate buffer

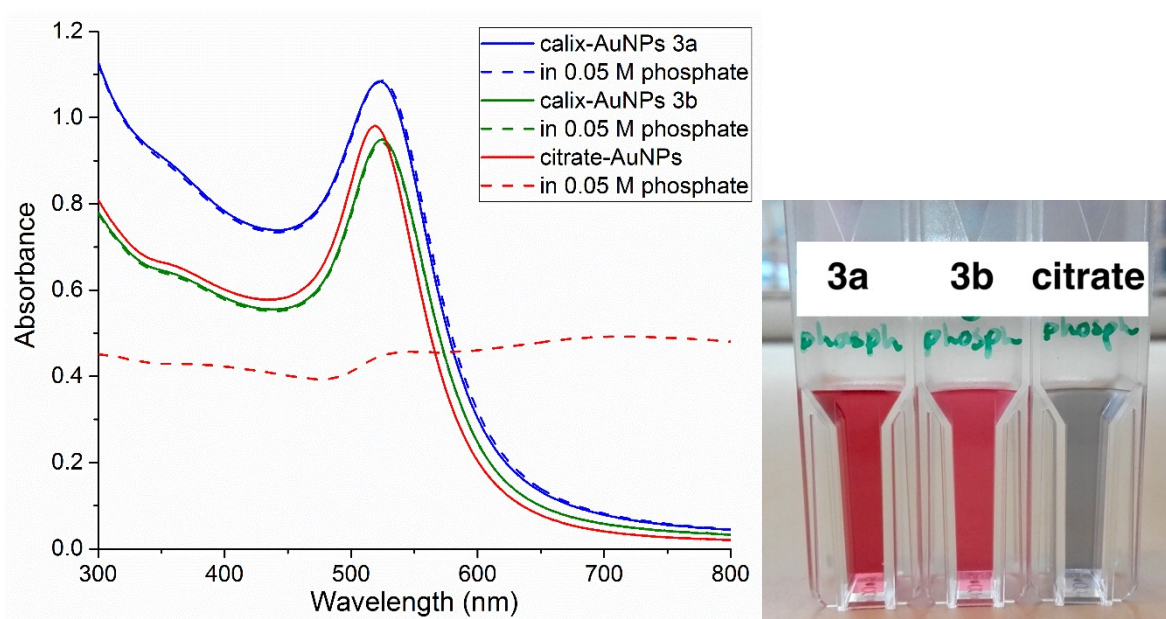


**Figure S23.** UV-Visible spectra of dispersions of calix-AuNPs **3a** (blue), calix-AuNPs **3b** (red), and 15 nm AuNPs in 1 mM citrate (green) in water (solid lines) and in 0.05 M phosphate buffer at pH 7.4 (dashed lines), showing strong aggregation of the citrate-protected AuNPs in buffer solution, whereas calixarene-functionalized AuNPs **3a** and **3b** remain stable. The photo shows the AuNP dispersions in phosphate buffer.



## 8. Post-functionalization of calix[4]arene-stabilized AuNPs **3a** by EDC/NHS coupling.

1 mL of the calix[4]arene stabilized AuNP **3a** dispersion was first neutralized by the addition of 1 mL of 1M HCl solution. 0.2 mL of aqueous EDC solution ( $1 \text{ mol.L}^{-1}$ ) was then added and the suspension was stirred 1 hour before the addition of 0.4 mL of a NHS aqueous solution ( $1 \text{ mol.L}^{-1}$ ). This mixture was then stirred another hour. 50 mg of dodecylamine (or undec-10-ynyl-1-amine<sup>11</sup>) was dissolved in 1 mL of THF and was added to the AuNP suspension. The reaction mixture was stirred another two hours, during which gold nanoparticles became progressively insoluble in the  $\text{H}_2\text{O}:\text{THF}$  mixture. 10 mL of ethanol were added to the suspension, which was then centrifugated at 7000 rpm for 10 min. Centrifugation cycles with ethanol were performed at least 5 times to purify the functionalized AuNPs. Post-functionalized AuNPs were soluble in  $\text{Et}_2\text{O}$  and exhibits a sharp localized resonance plasmon band centered at  $\lambda = 522 \text{ nm}$ .

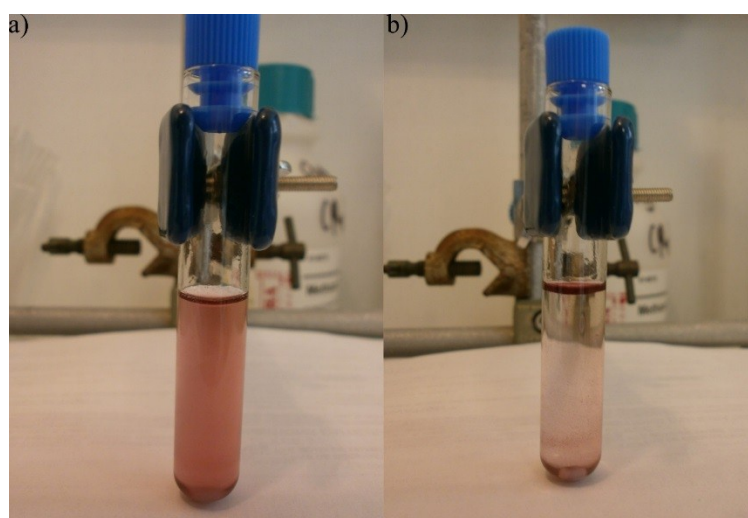


**Figure S24.** Photography of the reaction mixture of calix-AuNPs **3a** during post-functionalization experiments with dodecylamine at (a)  $t = 0$  and (b)  $t = 1\text{h}$ .

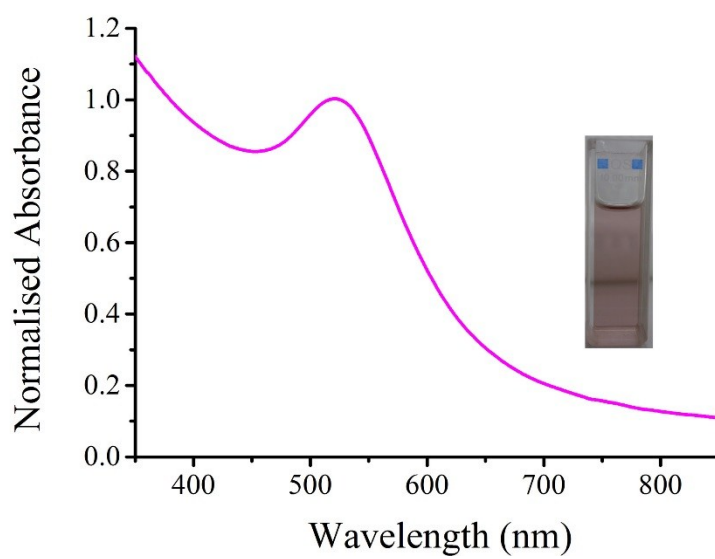


**Figure S25.** UV-Vis spectrum of post-functionalized AuNPs with dodecylamine dissolved in  $\text{Et}_2\text{O}$ . Insert: Photography of the solution.

## References.

---

- <sup>1</sup> A. Mattiuzzi, I. Jabin, C. Mangeney, C. Roux, O. Reinaud, L. Santos, J.-F. Bergamini, P. Hapiot and C. Lagrost, *Nat. Commun.*, 2012, **3**, 1130.
- <sup>2</sup> M. Doyen, K. Bartik and G. Bruylants, *J. Colloid Interface Sci.*, 2013, **399**, 1–5.
- <sup>3</sup> M. Doyen, J. Goole, K. Bartik and G. Bruylants, *J. Colloid Interface Sci.*, 2016, **464**, 160–166.
- <sup>4</sup> F. Mirkhalaf, J. Paprotny and D. Schiffrin, *J. Am. Chem. Soc.*, 2006, **128**, 7400-7401.
- <sup>5</sup> N. Griffete, H. Li, A. Lamouri, C. Redeuilh, K. Chen, C.-Z. Dong, S. Nowak, S. Ammar and C. Mangeney, *J. Mater. Chem.*, 2012, **22**, 1807-1811.
- <sup>6</sup> K. Kawai, T. Narushima, K. Kaneko, H. Kawakami, M. Matsumoto, A. Hyono, H. Nishihara and T. Yonezawa, *Appl. Surf. Sci.*, 2012, **262**, 76-80.
- <sup>7</sup> V. K. Ratheesh Kumar and K. R. Gopidas, *Chem. Asian J.*, 2010, **5**, 887-896.
- <sup>8</sup> M. Hashimoto, H. Toshima, T. Yonezawa, K. Kawai, T. Narushima, M. Kaga and K. Endo, *J. Biomed. Mat. Res. Part A*, 2014, **102A(6)**, 1838-1849.
- <sup>9</sup> S. Mondini, A. M. Ferretti, A. Puglisi and A. Ponti, *Nanoscale*, 2012, **4**, 5356–5372.
- <sup>10</sup> X. Liu, M. Atwater, J. Wang and Q. Huo, *Colloids and Surfaces B: Biointerfaces*, 2007, **58**, 3.
- <sup>11</sup> S. Butini, M. Brindisi, S. Gemma, P. Minetti, W. Cabri, G. Gallo, S. Vincenti, E. Talamonti, F. Borsini, A. Caprioli, M. A. Stasi, S. Di Serio, S. Ros, G. Borrelli, S. Maramai, F. Fezza, G. Campiani and M. Maccarrone, *J. Med. Chem.*, 2012, **55**, 6898–6915.